international journal of
powder metallurgy

Contents

50/1 **Winter 2014**

Cover: Microstructure of as-fabricated Ti-6Al-4V along the additive direction. *Photo courtesy H.P. Tang, Northwest Institute for Nonferrous Metal Research.*

The *International Journal of Powder Metallurgy* (ISSN No. 0888-7462) is a professional publication serving the scientific and technological needs and interests of the powder metallurgist and the metal powder producing and consuming industries. Advertising carried in the *Journal* is selected so as to meet these needs and interests. Unrelated advertising cannot be accepted.

Published quarterly by APMI International, 105 College Road East, Princeton, N.J. 08540-6692 USA. Telephone (609) 452-7700. Periodical postage paid at Princeton, New Jersey, and at additional mailing offices. Subscription rates to non-members—USA, Canada, and Mexico: $100.00 individuals, $255.00 institutions; overseas: additional $40.00 postage; single issues $60.00. Printed in USA. Postmaster: send address changes to the *International Journal of Powder Metallurgy*, 105 College Road East, Princeton, New Jersey 08540 USA USPS#267-120

ADVERTISING INFORMATION
Jessica Tamasi, APMI International
105 College Road East, Princeton, New Jersey 08540-6692 USA
Tel: (609) 452-7700 • Fax: (609) 987-8523 • E-mail: jtamasi@mpif.org

SELECTIVE ELECTRON BEAM MELTING OF TITANIUM AND TITANIUM ALUMINIDE ALLOYS

Huiping Tang,* Shenglu Lu, Wenpeng Jia,*** Guangyu Yang** and Ma Qian******

Selective electron beam melting (SEBM) with an additive-layer thickness ~100 μm has been used to fabricate two titanium alloys (Ti-6Al-4V♦ and Ti-6Al-2.75Sn-4Zr-0.4Mo-0.45Si-0.1Y♦, designated Ti600 in China) and two TiAl alloys (Ti-48Al-2Nb-2Cr♦♦ (TiAl), and Ti-45Al-7Nb-0.2W♦♦ (TiAl-7Nb)). The as-fabricated Ti-6Al-4V and Ti600 alloys showed excellent tensile properties. Both alloys displayed a full-columnar microstructure parallel to the additive solidification direction with the transverse section showing an increasingly coarse microstructure towards the bottom of each cuboidal sample. Fine yttrium oxide dispersoids were observed in the matrix of the as-fabricated Ti600 alloy. In order to utilize additive manufacturing (AM) for the two brittle TiAl alloys, an anneal-accompanied SEBM process was developed, which allowed thermal stresses to relax during the AM process. In addition, the formation of various types of defects during SEBM is briefly discussed.

♦*Compostion in w/o*
♦♦*Composition in a/o*

INTRODUCTION

AM (3D printing) uses 3D CAD data to fabricate parts of polymeric, metallic, ceramic, and organic materials in a layer-by-layer additive mode. Compared with conventional manufacturing processes, AM techniques offer several unique attributes including flexibility of design, new capabilities in alloy development, and significant saving of materials and time.[1] AM has been used to produce various intricate components that cannot be fabricated by conventional techniques.[2–4] In the context of AM of metals, laser engineered net shaping (LENS), selective laser melting (SLM), and SEBM are the primary technologies.[5,6] For metals, LENS, which is based on coaxial powder feeding, is flexible and efficient for the fabrication of large metallic structures, but produces a low-quality surface finish. SLM and SEBM are both suited for the precision forming of intricate components,[7] but SEBM offers two distinct advantages over SLM. First, SEBM uses an electron beam (EB) to melt precursor metal powders under high vacuum. This makes the process particularly suitable in the manufacturing of reactive metals such as titanium.[8] Second, EB heating offers the potential to preheat the metal powders up to 1,100°C due to its high scanning rate. This attribute is crucial for the fabrication of brittle metallic materials such as TiAl intermetallic alloys.[9,10]

In this study, SEBM of two titanium alloys and two TiAl intermetallic alloys was studied. The two titanium alloys were the benchmark Ti-6Al-4V alloy and a yttrium-containing commercial titanium alloy, Ti-6Al-2.75Sn-4Zr-0.4Mo-0.45Si-0.1Y (Ti600). The two TiAl intermetallic alloys were Ti-48Al-2Nb-2Cr (TiAl) and Ti-45Al-7Nb-0.2W (TiAl-7Nb). With the exception of Ti-6Al-4V, information on the SEBM of the other three alloys is either limited or not readily available. The experimental results of this study should enhance the understanding of AM of these alloys in combination with SEBM.

**Professor and Director, ***Research Scientist, State Key Laboratory of Porous Metal Materials, Northwest Institute for Nonferrous Metal Research, Xi'an, 710016, China; E-mail: hptang@c-nin.com, **PhD candidate, School of Materials and Metallurgy, Northeastern University, Shenyang 110819, China; and State Key Laboratory of Porous Metal Materials, Northwest Institute for Nonferrous Metal Research, Xi'an, 710016, China , ****Professor, RMIT University, School of Aerospace, Mechanical and Manufacturing Engineering, GPO Box 2476, Melbourne, VIC 3001, Australia*

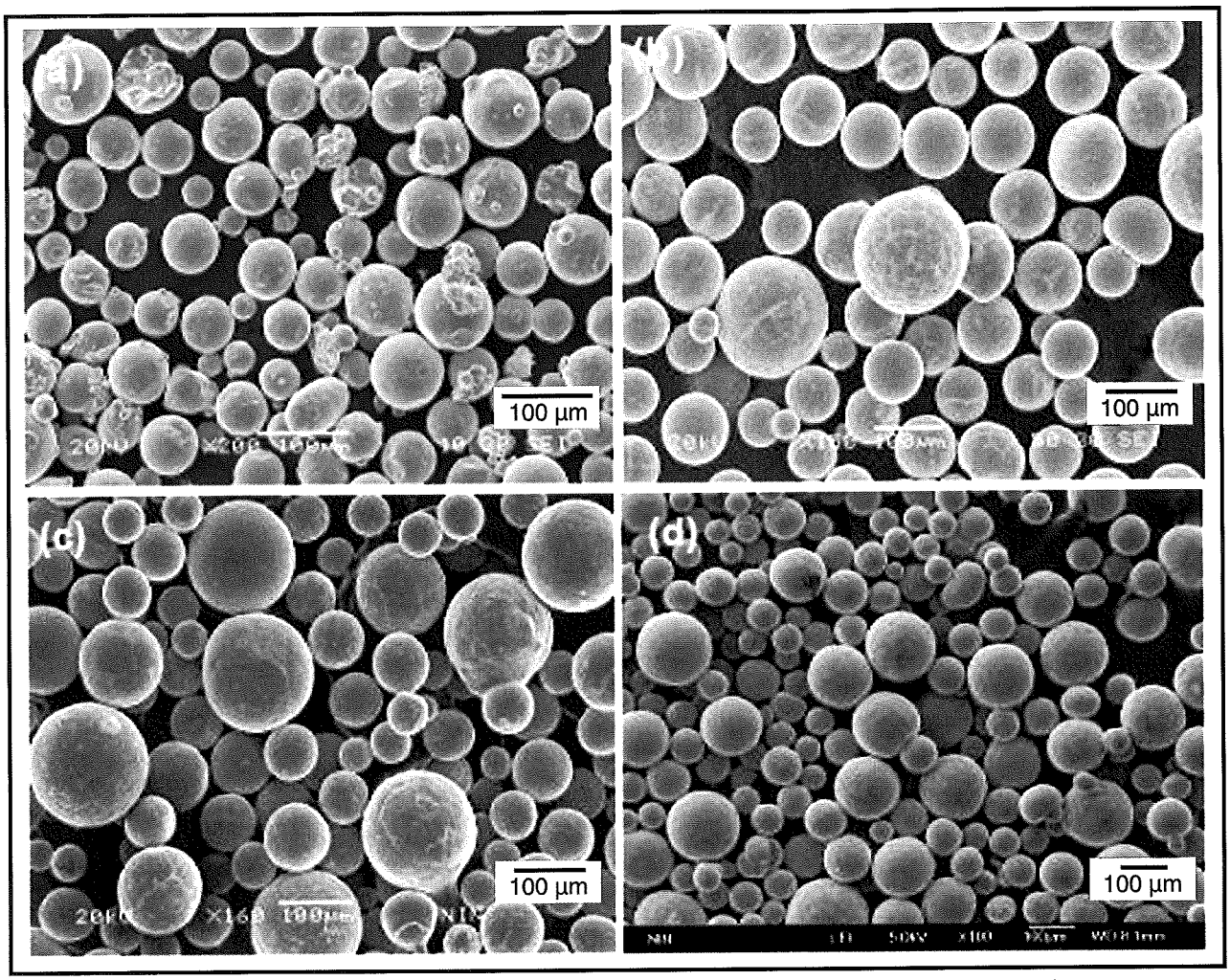

Figure 1. (a) Gas-atomized Ti-6Al-4V powder, (b) PREP Ti600 powder, (c) PREP Ti-48Al-2Nb-2Cr powder, and (d) PREP TiAl-7Nb powder

EXPERIMENTAL

Cuboidal samples (20 × 20 × 50 mm) of Ti-6Al-4V, Ti-6Al-2.75-Sn-4Zr-0.4Mo-0.45Si-0.1Y (Ti600), Ti-48Al-2Nb-2Cr (TiAl), and Ti-45Al-7Nb-0.2W (TiAl-7Nb) were fabricated using a 3 kW SEBM system (EBSM-250). The additive-layer thickness was ~100 µm and the scanning speed used for preheating the powder bed was 6–8 m/s. The EB current was varied in the range of 0.5 mA–20 mA, depending on the alloy. The EB current used for melting the powder was 10 mA with the melting speed set in the range of 1.5 m/s–5 m/s. Gas-atomized Ti-6Al-4V powder and Ti600, TiAl, and TiAl-7Nb powders produced by the plasma rotating electrode process (PREP), in the size range of 40–150 µm, were used. Figure 1 shows scanning electron micrographs (SEM) of the morphology of each powder used in this study.

The preheating temperatures used were 750°C for Ti-6Al-4V, 850°C for Ti600, and 1,050°C for both Ti-48Al-2Nb-2Cr and TiAl-7Nb. After preheating, the powder bed was selectively scanned to create a layer of cross section of the cuboidal part. The powder bed was then lowered and a fresh layer of powder spread on the building zone. The SEBM process was repeated until the last layer of the part was completed.

Samples for metallographic examination were cut from the as-fabricated cuboids and ground using silicon carbide papers down to 2400 mesh. They were then polished with a 0.05 µm Al_2O_3 suspension. Microstructures were characterized using optical microscopy (OM), scanning electron microscopy (SEM)

TABLE I. CHEMICAL COMPOSITIONS OF PA Ti-6Al-4V POWDER AND SEBM-FABRICATED Ti-6Al-4V SAMPLES

Element (w/o)	Ti	Al	V	O	N	H	C	Fe
PA Ti-6Al-4V Powder	Balance	6.46	4.13	0.09	0.02	0.002	0.02	0.2
SEBM-Fabricated Ti-6Al-4V	Balance	6.18	4.13	0.09	0.02	0.002	0.02	0.2

and transmission electron microscopy (TEM). The samples for characterization by OM and SEM were etched with a solution of modified Kroll's reagent (5 v/o HF, 15 v/o HNO_3, and 80 v/o H_2O), while those for TEM analysis were prepared by twin-jet polishing in a solution of 8 v/o perchloric acid and 92 v/o ethanol.

Tensile testing of the as-fabricated Ti-6Al-4V and Ti600 alloys was performed on an Instron 5982 testing machine at room temperature with a crosshead speed of 0.5 mm/min. Tensile specimens (3 mm diameter cross section and 15 mm gage length) were machined from the as-fabricated cuboids. A video extensometer was used to record the displacement.

RESULTS AND DISCUSSION

Microstructure and Mechanical Properties of SEBM-Fabricated Ti-6Al-4V

Table I lists the chemical compositions of both the prealloyed (PA) Ti-6Al-4V powder and the SEBM-fabricated Ti-6Al-4V alloy. No increase in the impurity content was detected after the SEBM process due to the vacuum condition used (10^{-2}–10^{-3} Pa). However, the aluminum content decreased noticeably from 6.46 w/o to 6.18 w/o because of the high-vacuum and high-temperature processing conditions. Hence, it is necessary to pre-compensate for this loss in alloy design.

A major issue encountered during SEBM is that, once created, the small molten pool (<200 μm in size) tends to spheroidize when the scanning electron beam moves forward, driven by surface tension. This often leads to the breakdown of the melt tracks and conglomeration of the powder particles. As a consequence, a variety of defects may develop, including porosity (due to conglomeration of powder particles) and improperly melted zones (due to the non-uniform particle-size distribution and the conglomeration of particles). These defects affect both the surface finish and the mechanical properties. To ensure smooth and consistent layer-additive build-up, and to avoid the formation of such defects, it is essential to control the surface temperature, EB scanning speed and overlapping timing, and positions of the EB scan lines. Figure 2 shows a transverse section of an SEBM-fabricated Ti-6Al-4V cuboidal sample. Non-destructive ultrasonic testing revealed no detectable pores or cracks consistent with the OM examination.

Figure 3 shows the microstructure of an SEBM-fabricated Ti-6Al-4V cuboid along the additive direction (longitudinal). Columnar structures are observed parallel to the additive direction while the transverse section shows an increasingly coarse microstructure from the top to the bottom due to the initial preheating and subsequent cyclic thermal effects (Figure 4).

Table II lists the tensile properties of the as-fabricat-

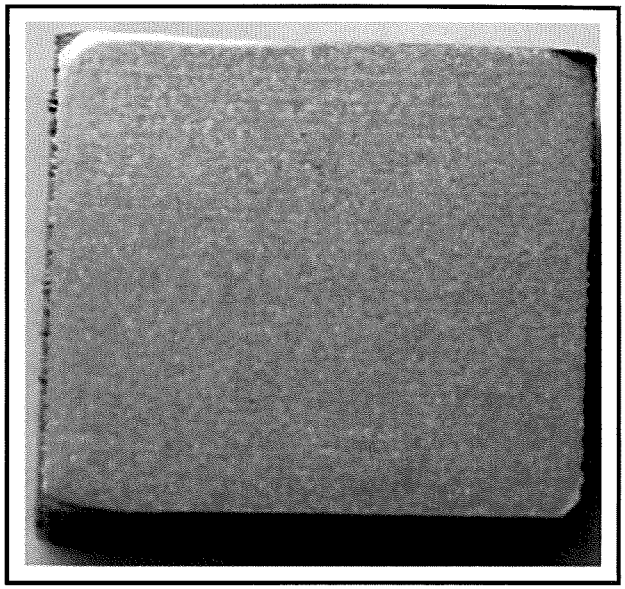

Figure 2. *Photograph of transverse section (20 x 20 mm) of SEBM-fabricated Ti-6Al-4V cuboid*

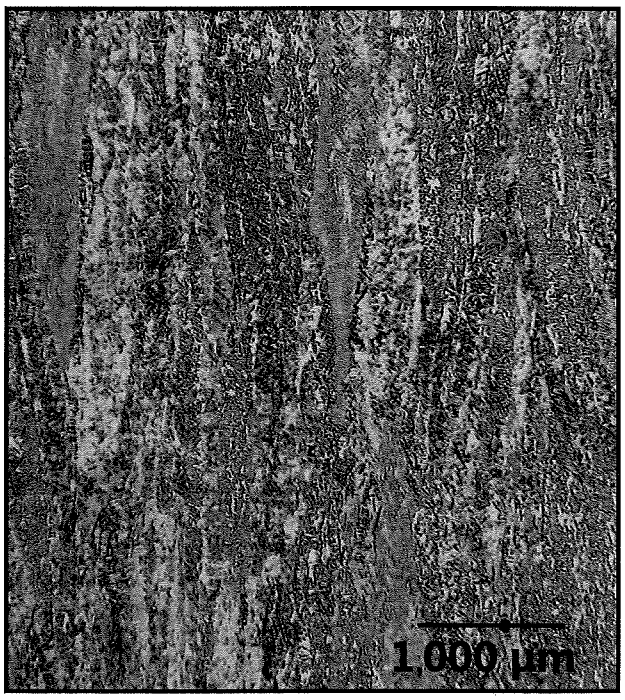

Figure 3. *Full-columnar microstructure of as-fabricated Ti-6Al-4V along the additive direction (OM)*

TABLE II. TENSILE PROPERTIES OF SEBM-FABRICATED Ti-6Al-4V ALLOY

	Yield Strength (MPa)	Ultimate Tensile Strength (MPa)	Reduction of Area (%)	Elongation (%)
Ti-6Al-4V	850	920	46.1	13.9
ASTM B381-10	828	895	25	10

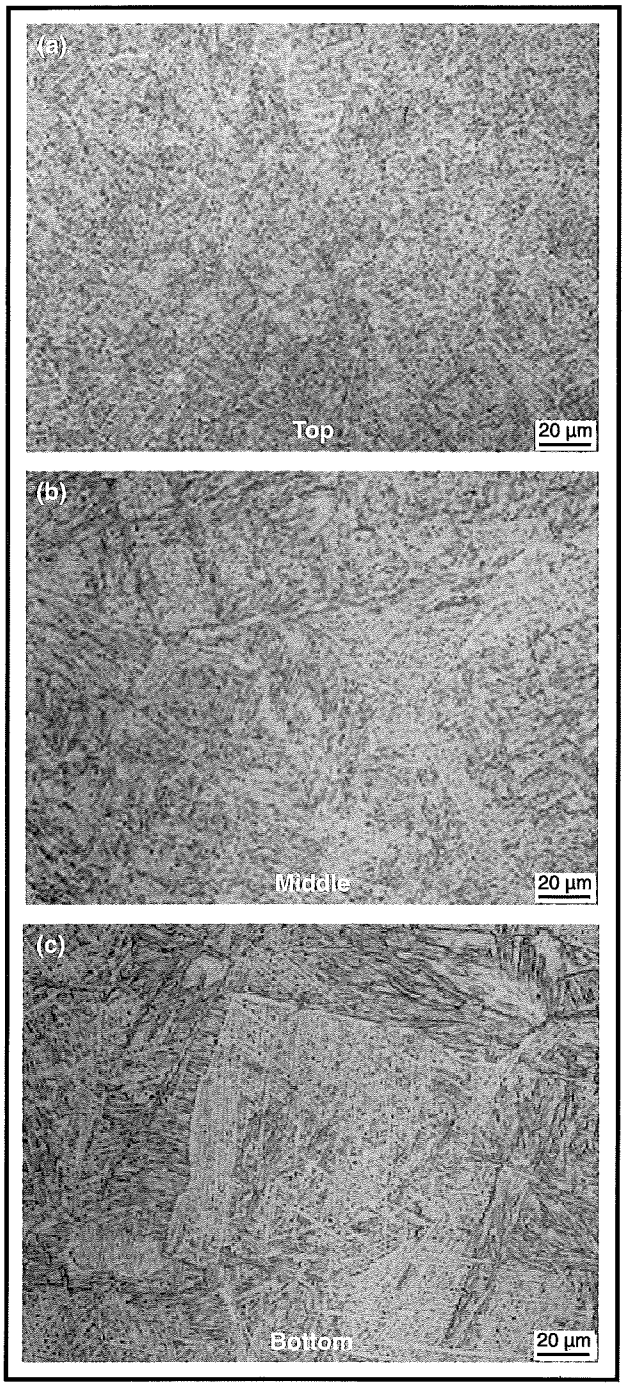

Figure 4. *Transverse section of microstructure from top to bottom of the cuboidal sample (OM)*

ed Ti-6Al-4V alloy; these properties meet the ASTM B381-10 standard specifications for Ti-6Al-4V forgings. The fractured surface shows ductile fracture characteristics, namely, dimpled ruptures, Figure 5.

Microstructure and Mechanical Properties of SEBM-Fabricated Ti600 Alloy

Similar to Ti-6Al-4V, the as-fabricated Ti600 alloy

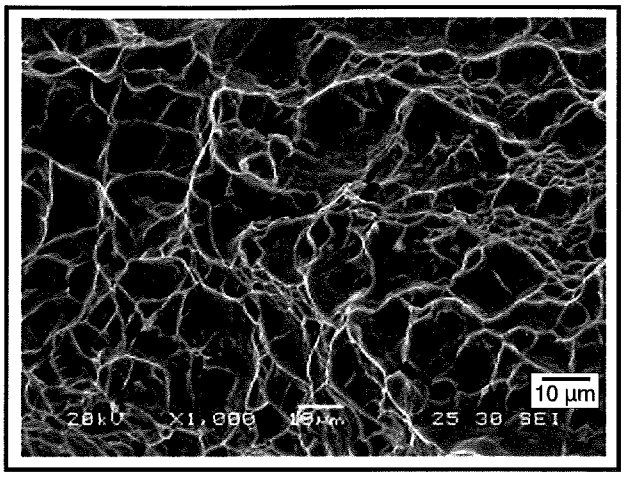

Figure 5. *Tensile-fracture surface of as-fabricated Ti-6Al-4V alloy (SEM)*

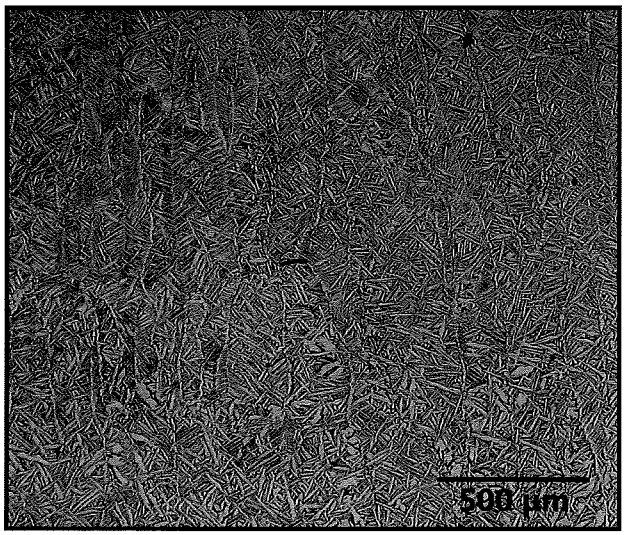

Figure 6. *Full-columnar microstructure of as-fabricated Ti600 parallel to the additive direction (OM)*

shows a full-columnar microstructure parallel to the additive direction (Figure 6) while the transverse section displays an increasingly coarse microstructure towards the bottom (Figure 7). Compared with most commercial titanium alloys, Ti600 contains 0.1 w/o Y. Figure 8(a) shows the fine precipitates observed in the α-matrix in the as-fabricated Ti600 alloy.

EDS spot analyses indicate that the precipitates are enriched in both Y and O (Figure 8 (b)), containing up to 12.36 a/oY and 23.43 a/o O. Y is a potent oxygen scavenger for titanium and forms a variety of yttrium oxides with different ratios of Y:O through a diffusion-controlled process but with the same lattice structure as Y_2O_3.[11,12] Hence, these fine dispersoids can be identified as Y_aO_b ($a \leq 2$ and $b \leq 3$) particles. They result in dispersion strengthening of the alloy. The ultimate tensile strength and yield strength of the as-fabricated Ti600 samples were 985 MPa and 943 MPa, respectively.

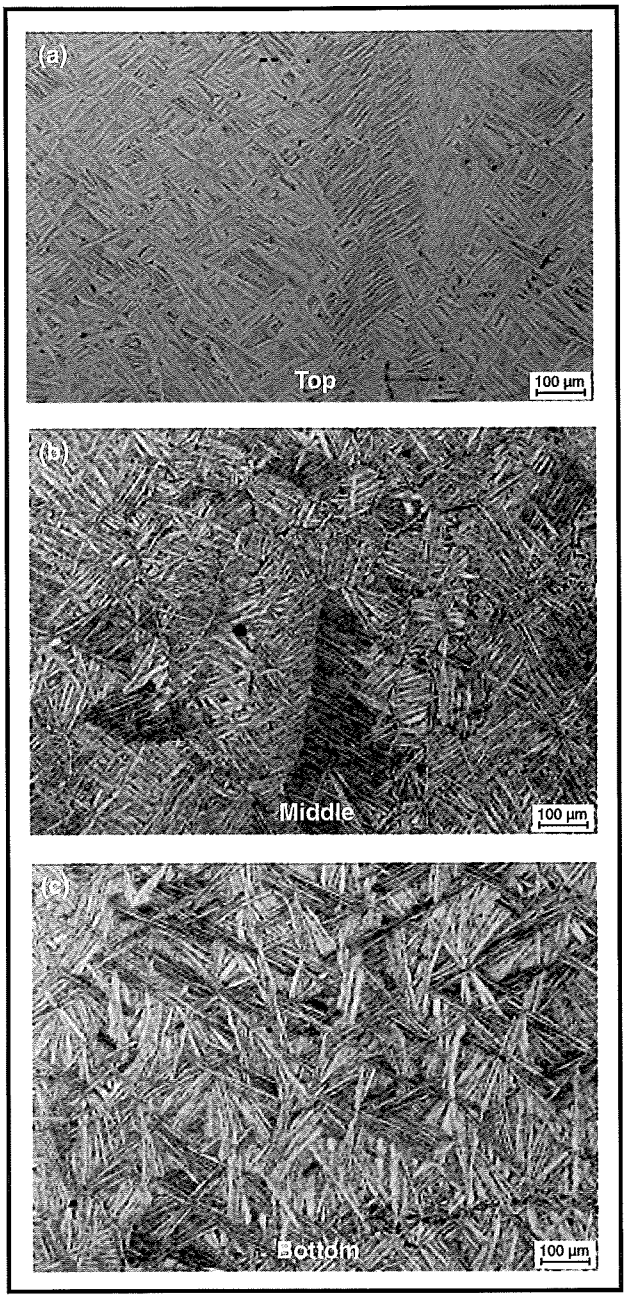

Figure 7. Transverse-section microstructures of SEBM-fabricated Ti600 alloy. The microstructure is much coarser at the bottom than at the top of the cuboid sample (OM)

Massive Transformation in SEBM-Fabricated Ti-45Al-7Nb-0.2W

Ti-45Al-7Nb-based alloys undergo massive transformations from α to γ on rapid cooling from the α-phase region.[13,14] The SEBM process is characterized by a relatively high cooling rate. As a result, massive transformations of α to γ occur during subsequent cooling following solidification, Figures 9 (a) and (b). Since SEBM is a layer-additive manufacturing process, each existing layer is subjected to the thermal effects arising from the build-up of the subsequent layers. Consequently, the massively formed γ-phase regions decompose into fine lamellar microstructures of α_2 and the stable γ-phases, Figures 9 (c) and (d). This differs from the coarse microstructure of as-cast Ti-45Al-7Nb-0.2W. Thus, the SEBM process offers a unique means of producing fine microstructures in γ-TiAl-based alloys.

Microstructures and Thermal-Stress Control in Ti-48Al-2Nb-2Cr

Microstructures of the SEBM-fabricated Ti-48Al-2Nb-2Cr alloy are shown in Figure 10. Microstructural constituents are lamellar colonies of α_2 + γ (grey), γ-phase (dark), and the B2-phase (light, Figure 10 (d)). Due to the cyclic thermal effects, the lamellar colonies of α_2 + γ at the bottom of the cuboidal specimens are coarser than those at the top. In addition, the microstructure changes from fully lamellar (top, Figure 10 (a)) to nearly lamellar (middle, Figure 10 (b)), and then to duplex microstructures (bottom, Figure 10 (c)). Also, the amount of the γ-phase tends to increase towards the bottom of the cuboidal specimen.

TiAl intermetallic alloys are difficult to fabricate due to their brittleness at room temperature. Thus, control of the thermal stresses is the key to their fabrication by SEBM. For this reason, an anneal-accompanied SEBM process, which includes preheating the powder bed to 1,050°C and maintaining this temperature during SEBM, has been developed. This procedure avoided the thermal stress that accumulates to a destructive level during SEBM and therefore enabled successful AM of the Ti-48Al-2Nb-2Cr alloy. In contrast, the Ti-48Al-2Nb-2Cr alloy fabricated without the accompanying anneal contained both macro- and micro-cracks. TEM analysis showed a variety of dislocation substructures in the Ti-48Al-2Nb-2Cr alloy fabricated by the anneal-accompanied SEBM process, Figure 11. Formation of these substructures is related to stress relaxation, but further studies are required to clarify this postulate.

SUMMARY

- SEBM-fabricated Ti-6Al-4V and Ti-6Al-2.75-Sn-4Zr-0.4Mo-0.45Si-0.1Y alloys showed a full-columnar microstructure along the additive (longitudinal) direction. In the transverse direction, an increasingly coarse microstructure developed towards the bottom due to cyclic thermal effects. However, both alloys showed excellent tensile properties in the as-fabricated state.
- Fine yttrium oxide (Y_aO_b) dispersoids were observed in the microstructure of the SEBM-fabricated Ti-6Al-2.75-Sn-4Zr-0.4Mo-0.45Si-0.1Y alloy.
- SEBM accompanied by annealing allows the thermal

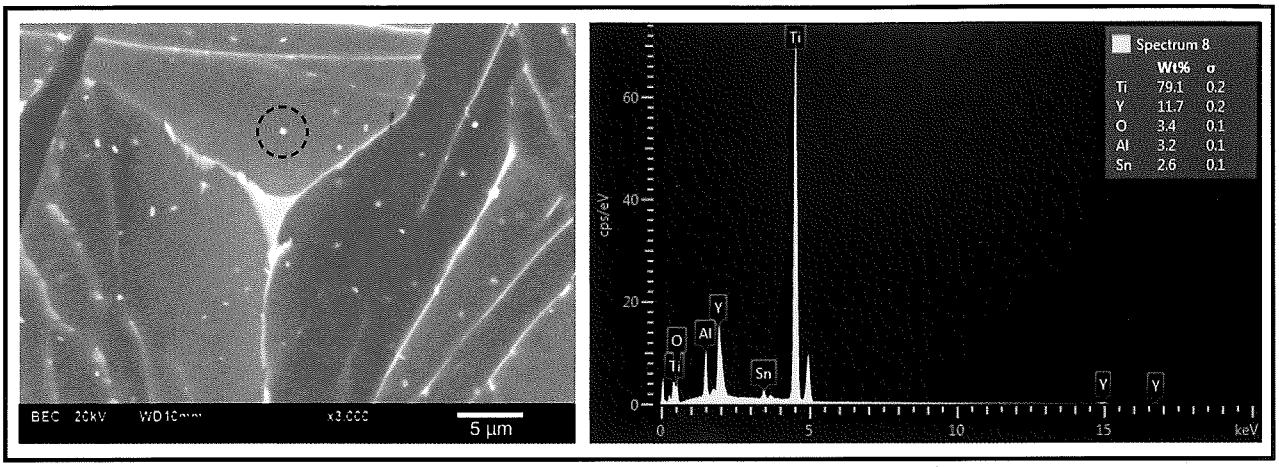

Figure 8. *(a) SEM backscattered electron (BSE) image showing fine dispersoids in α-matrix of as-fabricated Ti600 alloy containing 0.1 w/o Y. (b) EDS spectrum of precipitate particle shown in (a). The results indicate that the precipitates are Y- and O-enriched, containing up to 12.36 a/oY and 23.43 a/o O*

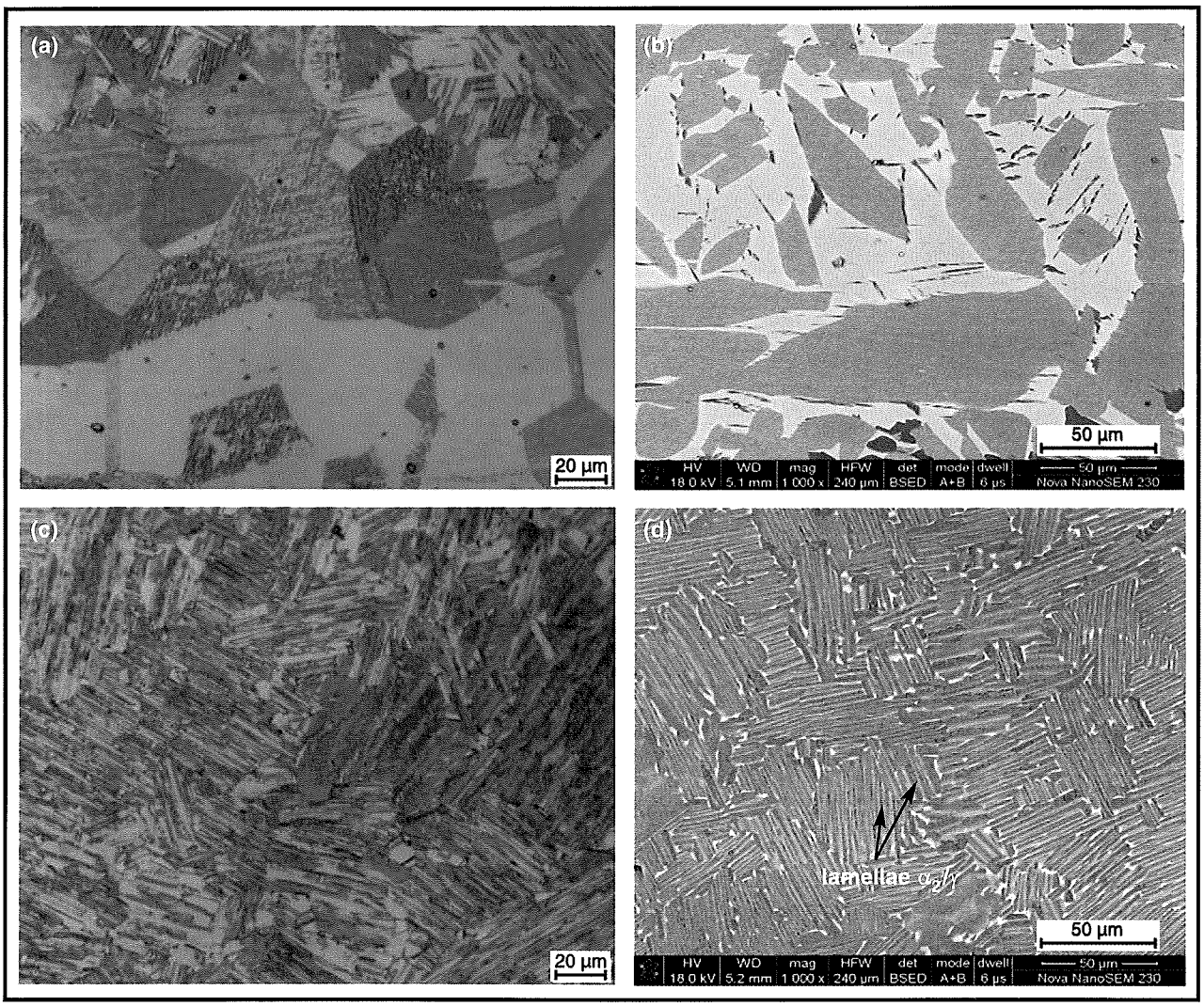

Figure 9. *Massively formed γ-phase regions (a) (OM) and (b) (SEM BSE). (c) (OM) and (d) (SEM BSE) fine lamellar microstructures of α_2 and the stable γ-phases in SEBM-fabricated Ti-45Al-7Nb-0.2W*

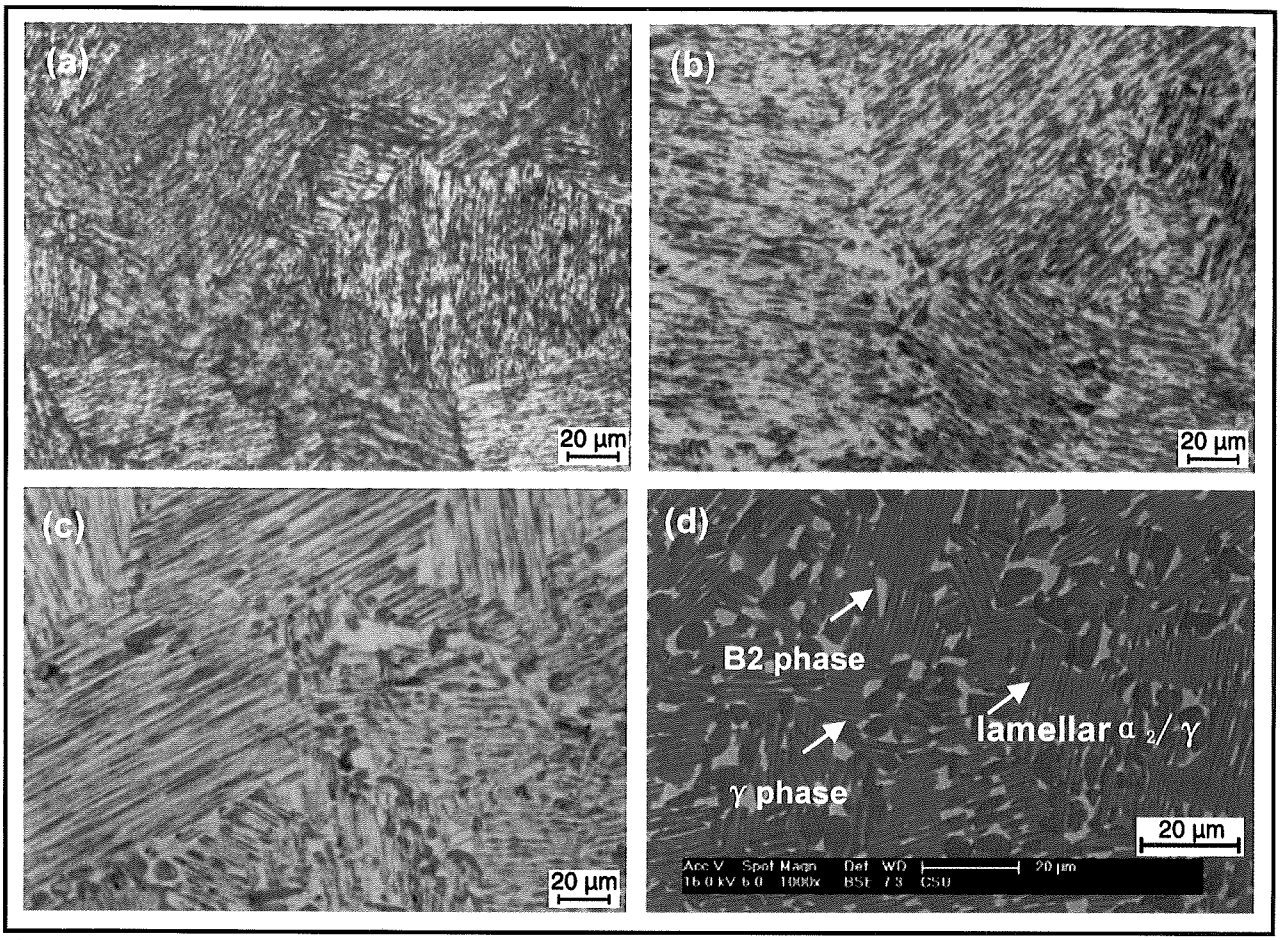

Figure 10. Optical microstructures of SEBM-fabricated Ti-48Al-2Nb-2Cr. (a) at the top, (b) middle, and (c) bottom of cuboidal sample. (d) SEM BSE micrograph showing phases present in (c)

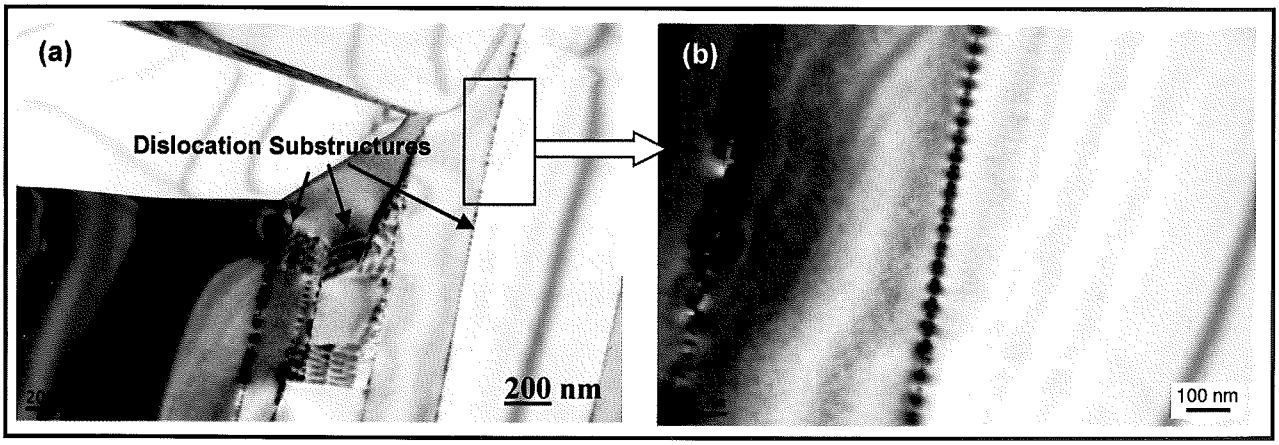

Figure 11. TEM bright field images of dislocation substructures in Ti-48Al-2Nb-2Cr fabricated by the anneal-accompanied SEBM process

stresses to relax during AM. This enables the quality fabrication of the Ti-45Al-7Nb-0.2W intermetallic alloy by SEBM. Without the accompanied annealing, cuboidal samples of the alloy fabricated by SEBM contained both macro- and micro-cracks.

- A massive transformation of α to γ occurred in the Ti-45Al-7Nb-0.2W alloy during SEBM. However, due to the subsequent cyclic thermal effects, the γ-phase regions decomposed into fine lamellar microstructures of α_2 and stable γ-phases. Thus, the massive transformation offers a unique means of microstructural control with SEBM.

ACKNOWLEDGEMENTS

This work was supported by the International Science and Technology Cooperation Programme (NO.2011DFA52590) of the Ministry of Science and Technology China and the National High Technology Research Program (No. 2013AA031103).

REFERENCES

1. E.M. Sachs, M.J. Cima and P. Williams, "Three Dimensional Printing: Rapid Tooling and Prototypes Directly from a CAD Model", *J. Eng. Ind.*, 1992, vol. 114, no. 4, pp. 481–488.
2. P. Heinl, "Cellular Ti-6Al-4V Structures with Inter-Connected Macro Porosity for Bone Implants Fabricated by Selective Electron Beam Melting", *Acta Biomater.*, 2008, vol. 4, pp. 1,536–1,544.
3. A. Bandyopadhyay, B.V. Krishna and W.C. Xue, "Application of Laser Engineered Net Shaping (LENS) to Manufacture Porous and Functionally Graded Structures for Load Bearing Implants", *J. Mater. Sci: Materials in Medicine,* 2009, vol. 20, pp. 29–34.
4. K.N. Amato, "Microstructures and Mechanical Behavior of Inconel 718 Fabricated by Selective Laser Melting", *Acta Mater.*, 2012, vol. 60, pp. 2,229–2,239.
5. Y.Q. Yang, F. Lin and H.B. Qiao, "Overview of Direct Metal Rapid Prototyping and Manufacture Ring Technology", *Chin. J. Mech. Eng.*, 2005, vol. 43, no. 11, pp. 1–6.
6. Y.Q. Yang, Y. Liun, C.H. Song , "The Status and Progress of Manufacturing of Metal Parts by 3D Printing Technology", *Chin. J. Mech. Eng.*, 2013, vol. 42, no. 4, pp. 1–5.
7. M. Koike, P. Greer and P. Owen, "Evaluation of Titanium Alloys Fabricated Using Rapid Prototyping Technologies—Electron Beam Melting and Laser Beam Melting", *Acta Mater.*, 2011, vol.4, pp. 1,776–1,792.
8. M. Koike, K. Martinez and L.L. Guo, "Evaluation of Titanium Alloy Fabricated using Electron Beam Melting System for Dental Applications", *J. Mater. Pro, Tech.*, 2011, vol. 211, pp. 1,400–1,408.
9. D. Srivastava, "Microstructural Characterization of the γ-TiAl Alloy Samples Fabricated by Direct Laser Fabrication Rapid Prototype Technique", *Bull. Mater. Sci.*, 2002, vol. 25, no. 7, pp. 619–633.
10. S. Biamino, A. Penna and U. Ackelid, "Electron Beam Melting of Ti48Al2Cr2Nb Alloy: Microstructure and Mechanical Properties Investigation", *Intermetallics,* 2011, vol. 19, pp. 776–781.
11. M. Yan, Y. Liu, Y.B. Liu, C. Kong, G.B. Schaffer and M. Qian, "Simultaneous Gettering of Oxygen and Chlorine and Homogenization of the β Phase by Rare Earth Hydride Additions to a Powder Metallurgy Ti-2.25Mo-1.5Fe Alloy", *Scripta Mater.*, 2001, vol. 67, pp. 491–494.
12. M. Yan, Y. Liu, G.B. Schaffer and M. Qian, "In-situ Synchrotron Radiation to Understand the Pathways for the Scavenging of Oxygen in Commercially-Pure Ti and Ti-6Al-4V by Yttrium Hydride", *Scripta Mater.*, 2013, vol. 68, pp. 63–66.
13. H. Saage, A.J. Huang, D. Hu, M.H. Loretto and X. Wu, "Microstructures and Tensile Properties of Massively Transformed and Aged Ti46Al8Nb and Ti46Al8Ta Alloys", *Intermetallics,* 2009, vol. 17, pp. 32–38.
14. V. Imayev, T. Khismatullin, T. Oleneva, R. Imayev, R. Valiev, R. Wunderlich, A. Minkow, U. Hecht and H.J. Fecht. "Grain Refinement in Cast Ti-46Al-8Nb and Ti-46Al-8Ta Alloys via Massive Transformation", *Adv. Eng. Mater.*, 2008, vol. 10, pp. 1,095–1,100.